SciEn
Journal of Engineering Advancements Vol. 05(01) 2024, pp 1-8 https://doi.org/10.38032/jea.2024.01.001

# Numerical Analysis of Laminar Natural Convection Inside Enclosed Squared and Trapezoidal Cavities at Different Inclination Angles

*Mohammad Sultan Mahmud**, *Md. Mahbubur Rahman*, *Md. Nahid Zaman Liton*

Department of Mechanical Engineering, Khulna University of Engineering & Technology, Khulna-9203, Bangladesh

Received: November 27, 2023, Revised: January 08, 2024, Accepted: January 16, 2024, Available Online: January 19, 2024

## ABSTRACT

The effects of cavity shape by inclination angle on laminar natural convection inside trapezoidal and square-shaped cavities have been numerically investigated in this work. Several simulations had been conducted for various inclinations of the trapezoidal cavity at Rayleigh numbers (Ra) $=10^5$ to $10^6$ in a laminar flow regime. The walls at the left and right sides of the cavities were heated isothermally, while the walls at the top and bottom sides were adiabatic. The problem was assumed to be 2-D and solved using the software package ANSYS Fluent 16.2. Cavity filled with air is examined in two distinct instances; varying boundary layers and the flow generated for the natural convection. This numerical study analyzed the flow characteristics, temperature distribution, and Nusselt number. The analysis reveals that as the Rayleigh number increases, the Nusselt number also increases, with a more pronounced effect at higher Rayleigh numbers. It has been observed that there is a substantial effect of cavity shapes on the Nusselt number. The presence of an angled wall inhibits convection resulting in stronger flow in the squared cavity compared to the trapezoidal cavity. From numerical results, it is also found that the temperature distribution at Ra = $10^5$ is wider than the temperature distribution at Ra= $10^6$.

Keywords: Natural Convection, Nusselt Number, Inclination Angle, Rayleigh Number, Laminar Flow.



## 1 Introduction

A specific type of flow known as natural convection occurs when a fluid, like air, moves across space because some of its constituent parts are heavier than others rather than because of external forces. Buoyancy is the driving force for free convection. Free convection occurs when a fluid encompassing a heat source absorbs heat and then becomes less dense and rises because of thermal expansion. Thermal expansion that is caused in the fluid is critical. In other words, a heavier component results in less dense components falling, while lighter components result in more dense components rising, resulting in bulk fluid movement.

Researchers are becoming highly interested in natural convection in enclosures because of its wide range of applications and significant influence on thermal characteristics. Since natural convection is employed in a wide range of technical applications, including geophysics, geothermal reservoirs, building insulation, industrial separation processes, and so forth, it has been studied inside a variety of enclosure shapes and with a variety of boundary conditions to investigate thermal behavior as well as fluid flow. In many engineering systems, as well as geophysical situations when the enclosure geometry fluctuates or has additional tending walls, any triangle, square, or rectangular hole is unsuitable. Because of the slanted walls, examining natural convection in a trapezoidal enclosure is significantly more challenging than in any other enclosure.

Some parameters, such as the enclosure's shapes, angle of inclination, aspect ratio, and Rayleigh number, govern natural heat transport characteristics inside the enclosures. An extensive investigation was carried out to determine the influence of enclosure Rayleigh number and aspect ratio. Adibi *et al.* [1] and De Vahl Davis [2] investigated the heat transport properties of a 2-D rectangular and trapezoidal enclosure with isothermal boundary conditions for various Rayleigh number and aspect ratios by using numerical methods. When the Rayleigh number exceeds specific threshold values, the fluid flow becomes turbulent because of the induced buoyancy. Sharif and Liu [3] investigated how various inclination angles affected turbulent convection in rectangular-shaped cavities. In two separate studies, Adibi and Razavi [4], [5] simulated spontaneous and forced convection in three different bench markings. The author's benchmarks were flow over a cylinder that is round and flow through a squared cavity, which is comprised of two parallel plates. They employed an innovative numbering scheme that they came up with on their own. Heat transport was studied numerically and experimentally by Akbari [6]. For numerical simulations, he used the finite difference method. Zaharudddin *et al.* [7] numerically investigated the natural convection driven by buoyancy and Marangoni effects within a right-angled trapezoidal-shaped cavity containing water-based nanofluids. Alshomrani *et al.* [8] investigated the effect of the cooler's placement, aspect ratio, and positioning of the heated solid object within the enclosure numerically on the three-dimensional natural convection flow. Yazdani *et al.* [9] carried out a computational analysis on an enclosure of a trapezoidal shape filled with a non-Newtonian fluid following a power-law behavior. Their study focused on heat transfer by natural convection within the enclosure and the resulting generation of entropy. Mote Gowda *et al.* [10] explored free convection within a trapezoidal-shaped enclosure featuring discrete heating. Reddy *et al.* [11] studied extensively the heat transfer phenomenon by natural convection originating from a heated cylinder positioned within a square-shaped cavity containing micro-polar fluid. Kishor *et al.* [12] conducted both numerical simulation and experimental work in vertically oriented closed cavities for an aspect ratio of three, utilizing air as the working fluid at various

*Corresponding Author Email Address: sultan@me.kuet.ac.bd 

temperature differences and Rayleigh numbers. Inam [13] investigated laminar natural convection in a square-shaped cavity at various inclination angles by direct numerical simulation. Ghalambaj *et al.* [14] explored the conjugate natural convection phenomenon within a square-shaped cavity using nanofluid while varying the volume fraction of the nanoparticles at different Rayleigh numbers and thermal conductivity ratio between wall and nanofluid. Nadim *et al.* [15] also performed a numerical investigation in a rectangular enclosure with a rotating object inside for a comprehensive analysis of fluid flow inside the field.

From the earlier literature review, it is observed that there is a less amount of research work on the effect of inclination angle (φ=0˚, φ=45˚, φ=50˚ and φ=60˚) of a trapezoidal-shaped cavity at considerably low Rayleigh number which was the motivation for current research work. Several simulations were performed for different inclination angles of a trapezoidal-shaped cavity at two Rayleigh numbers Ra = $10^5$ and Ra = $10^6$ using ANSYS Fluent 16.2. Natural convection in both trapezoid and squared-shaped cavities has been simulated in this work using numerical methods under various conditions. In this work, different geometry and different boundary conditions are examined, and results for these different conditions have been analyzed.

## 2 Methodology

The physical system of the problem has been illustrated in Fig. 1.

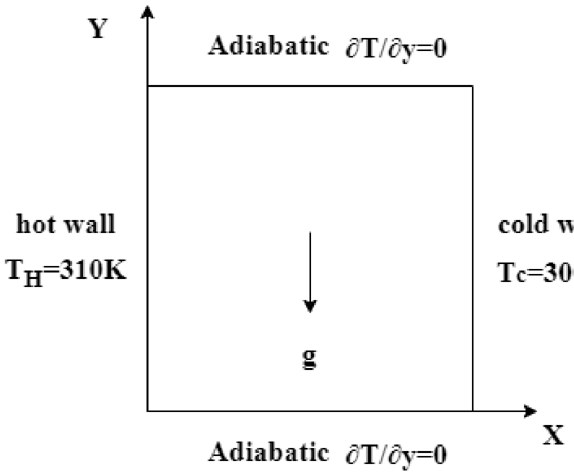


(a)

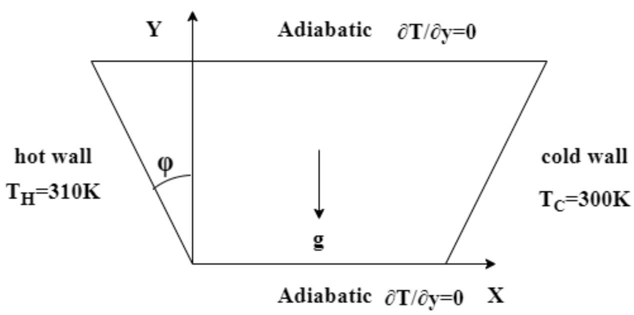


(b)

Fig. 1 Schematic diagram of the physical system for enclosed (a) square (φ=0˚) and (b) trapezoid (φ>0˚) cavities

This study considers two separate states. In the first case, the original environment is created in a squared-shaped cavity (φ=0˚). In this situation, the fluid in the cavity is termed air applied to the equation of state as the gas equation. The second case possesses similarity to the first one, but the shape of the cavity is trapezoidal (φ>0˚). Air is used as fluid inside the trapezoidal cavities in this case. Different angles of inclination (φ=45˚ to 60˚) at both sides of the cavities were used for simulation to monitor how the inclination angle affects the natural convection in the trapezoidal cavities. The temperature of the right cold wall is 300K, whereas the temperature of the left hot wall is 310K. The upper and lower walls were set adiabatic i.e. $\frac{\partial T}{\partial y} = 0$.

The numerical domain used for simulation was a two-dimensional square and trapezoid cavity with dimensions 200mm x 200mm containing air sketched in Fig. 2. The walls at the top and the bottom sides were set adiabatic, the slope of the trapezoid cavities has been changed. The Boussinesq approximation used for relating the temperature field to the flow field in the motion has been applied for simplifying the calculations of buoyancy due to density difference in the current study of natural convection heat transfer.

(a)

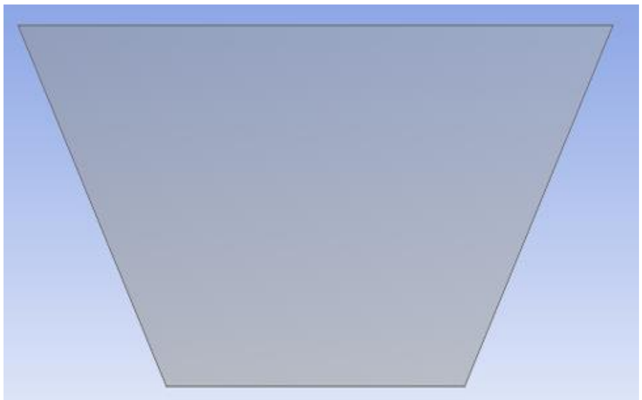

(b)

Fig. 2 Computational domain of (a) squared and (b) trapezoidal cavities for numerical simulation.

Fig. 3 shows the grids that were considered for the square and trapezoid. Because created boundary layers necessitate high-accuracy computations, the grids positioned alongside the walls are finer than those at locations further away from the walls.

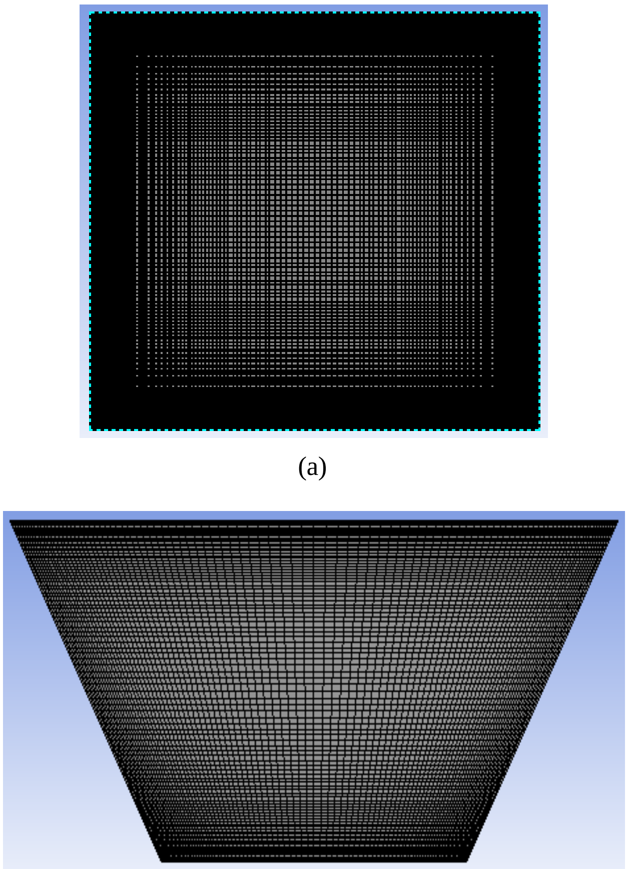

(a)

(b)

Fig. 3 Grid for (a) squared and (b) trapezoid cavities

The face sizing and edge sizing procedures are used to create the mesh. The grid size used in this simulation is 150x150. For better results of thermal performance, the meshing was done by using bias. For biasing, a bias factor value of 5 was used. Fig. 4 represents the mesh independency test result for the trapezoid cavities.

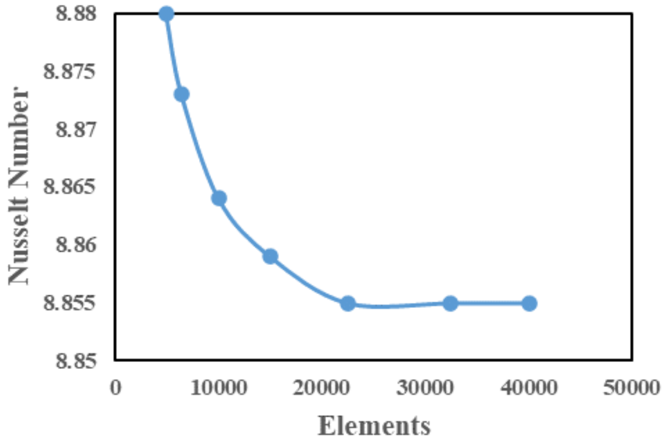


Fig. 4 Mesh independence test for the simulation work

In heat transfer at a boundary (surface) within a fluid, the Nusselt number (Nu) is the ratio of convective to conductive heat transfer across (normal to) the boundary.

$$Nu = \frac{Convective\ heat\ transfer}{conductive\ heat\ transfer} = \frac{h\,L}{k} \tag{1}$$

Where h is the convective heat transfer coefficient of the flow, L is the characteristic length, and k is the thermal conductivity of the fluid.

The Rayleigh number is a dimensionless number that is associated with buoyancy-driven airflow and can be regarded as a measure of the driving forces of natural convection.

Thus, the Rayleigh number is defined as

$$Ra = \frac{g\beta\rho^2 C_p \Delta T L^3}{\mu k} \tag{2}$$

Where g is the acceleration of gravity, β is the thermal expansion coefficient, ρ is the density of the fluid, ΔT is the temperature difference, L is the length of the enclosure, μ is dynamic viscosity and k is the thermal conductivity.

The progression of natural convection flows within the enclosure is governed by the following set of governing equations [16] using the Boussinesq approximation [17].

$$\frac{\partial u}{\partial x} + \frac{\partial v}{\partial y} = 0 \tag{3}$$

$$u\frac{\partial u}{\partial x} + v\frac{\partial u}{\partial y} = \frac{1}{\rho} - \frac{\partial P}{\partial X} + \left(\frac{\partial^2 u}{\partial x^2} + \frac{\partial^2 u}{\partial y^2}\right) \tag{4}$$

$$u\frac{\partial v}{\partial X} + v\frac{\partial v}{\partial y} = -\frac{1}{\rho}\frac{\partial P}{\partial y} + \left(\frac{\partial^2 v}{\partial x^2} + \frac{\partial^2 v}{\partial y^2}\right) + g\beta + (T - T_o) \tag{5}$$

$$u\frac{\partial T}{\partial x} + v\frac{\partial T}{\partial y} = k\left(\frac{\partial^2 T}{\partial x^2} + \frac{\partial^2 T}{\partial x^2}\right) \tag{6}$$

where $u$, $v$ are the velocity components in the x and y direction, respectively. ρ is the density of air. Also, $\vartheta$ and $k$ are kinematic viscosity and thermal diffusivity respectively. The volumetric thermal expansion coefficient is denoted by β and g represents the acceleration of gravity. The above equations (Eq. (3) to Eq. (6)) are numerically solved using the technique of finite volume method. The appropriate boundary conditions of the problem are:

For left wall: $u = v = 0$ & $T_H = 310K$

For right wall: $u = v = 0$ & $T_C = 300K$

For lower and upper walls: $u = v = 0$ & $\frac{\partial T}{\partial y} = 0$

The geometric models are solved by using ANSYS Fluent 16.2. For the residuals, the convergence criteria are set to$10^{-8}$ for the continuity equation, x-velocity and y-velocity equation, and energy equation. In solution initialization, the standard initialization approach was used, and solution initialization is necessary before the computation executes. It was repeated until the convergence requirements were met.

As indicated in Table 1, the current numerical simulation has been validated against solutions found in the literature. The average Nusselt number at the hot wall of the air-filled square cavity, as determined by many investigations, is displayed in Table 1 and contrasted with the results of the current investigation for varying Rayleigh numbers.

The Rayleigh number ranged from $10^3$ to $10^6$ in the laminar flow regime (a flow regime characterized by high momentum diffusion and low momentum convection) have been considered in the current analysis.

Table 1 Comparison of Nusselt number at the hot wall of the square cavity of the current work with previous works

| Rayleigh Number | Present study | Vahl Davis and Jones [18] | Fusegi et al. [19] | Khanafer et al. [20] | Billigen [21] | Lai and Yang [22] | Kobra et al. [23] |
|---|---|---|---|---|---|---|---|
| $10^3$ | 1.1179 | 1.118 | 1.105 | 1.118 | - | 1.126 | - |
| $10^4$ | 2.247 | 2.243 | 2.302 | 2.245 | 2.245 | 2.252 | 2.2448 |
| $10^5$ | 4.534 | 4.519 | 4.646 | 4.522 | 4.521 | 4.514 | 4.5216 |
| $10^6$ | 8.855 | 8.799 | 9.012 | 8.826 | 8.800 | 8.752 | 8.8262 |

## 3 Results and Discussion

Fig. 5 shows the contour showing the temperature of trapezoidal cavities for different shapes of geometry and for variation of inclination angle at Rayleigh number $10^6$. Fig. 5(a) depicts the temperature of trapezoid cavities for different angles φ = 45˚, φ = 50˚, φ = 60˚ respectively at Rayleigh number $10^6$. From all the figures, it is seen that the temperature close to the left wall is higher than the right wall. It is due to the higher temperature of the wall at the left which is 310K than the wall at the right which is 300K.

It is also seen that the temperature at the wall of the top side is larger than the temperature at the wall of the bottom side. It is because the temperature of the fluid close to the left wall is raised because of heating. Consequently, fluid density decreases. Then this warm air travels to the top wall which results in higher temperature near the top wall than the bottom wall. Again, the temperature close to the right wall is lower than the left wall because of buoyancy. For the cooling effect, fluid density increases near the right wall, and fluid becomes heavier and colder near the right wall. A similar observation was found in other open literature [13].

Fig. 6 illustrates the contour showing the temperature of trapezoid cavities for different shapes of geometry and for variation of inclination angle at Rayleigh number $10^5$.

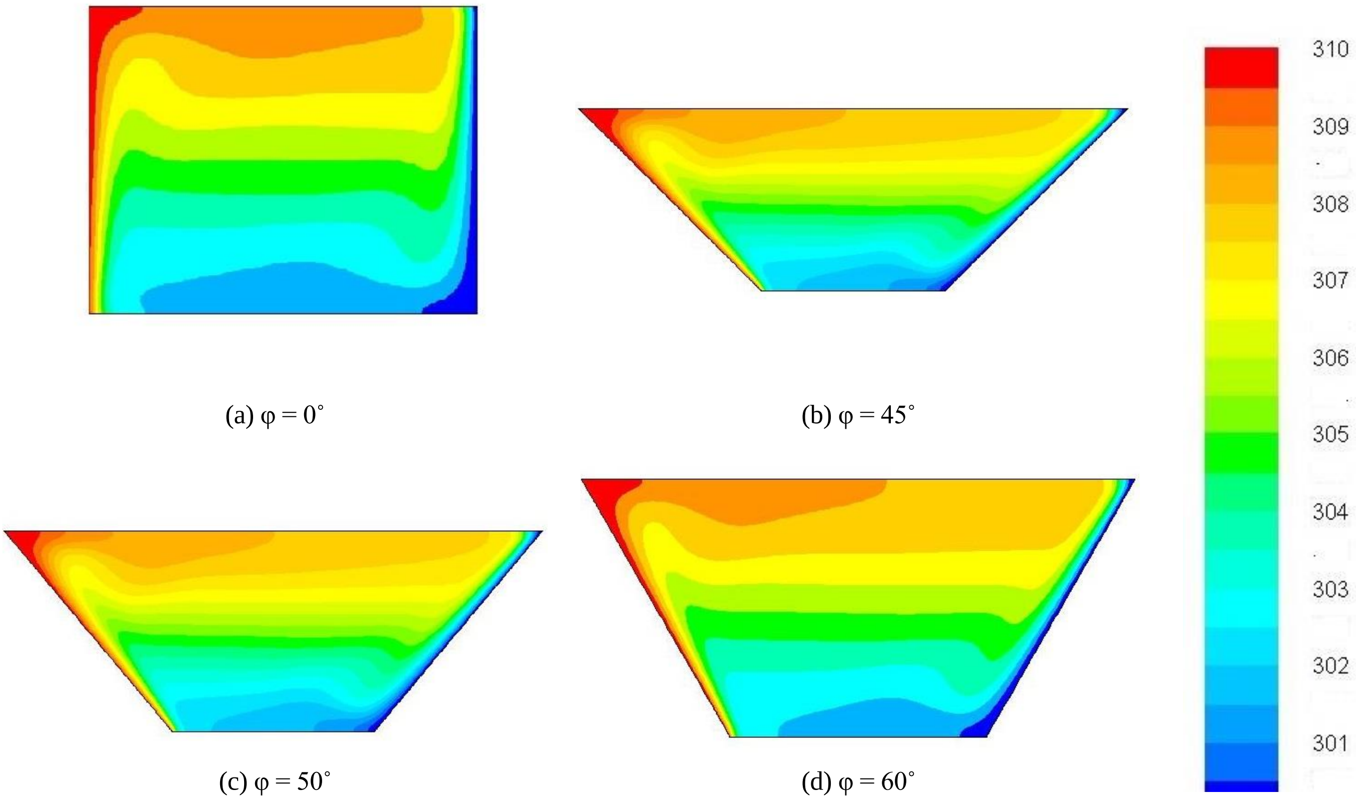


(a) φ = 0˚

(b) φ = 45˚

(c) φ = 50˚

(d) φ = 60˚

Fig. 5 Contour of the temperature of the square and trapezoid cavities for different inclination angles φ of (a) 0˚, (b) 45˚,(c) 50˚ and (d) 60˚at Ra = $10^6$

.

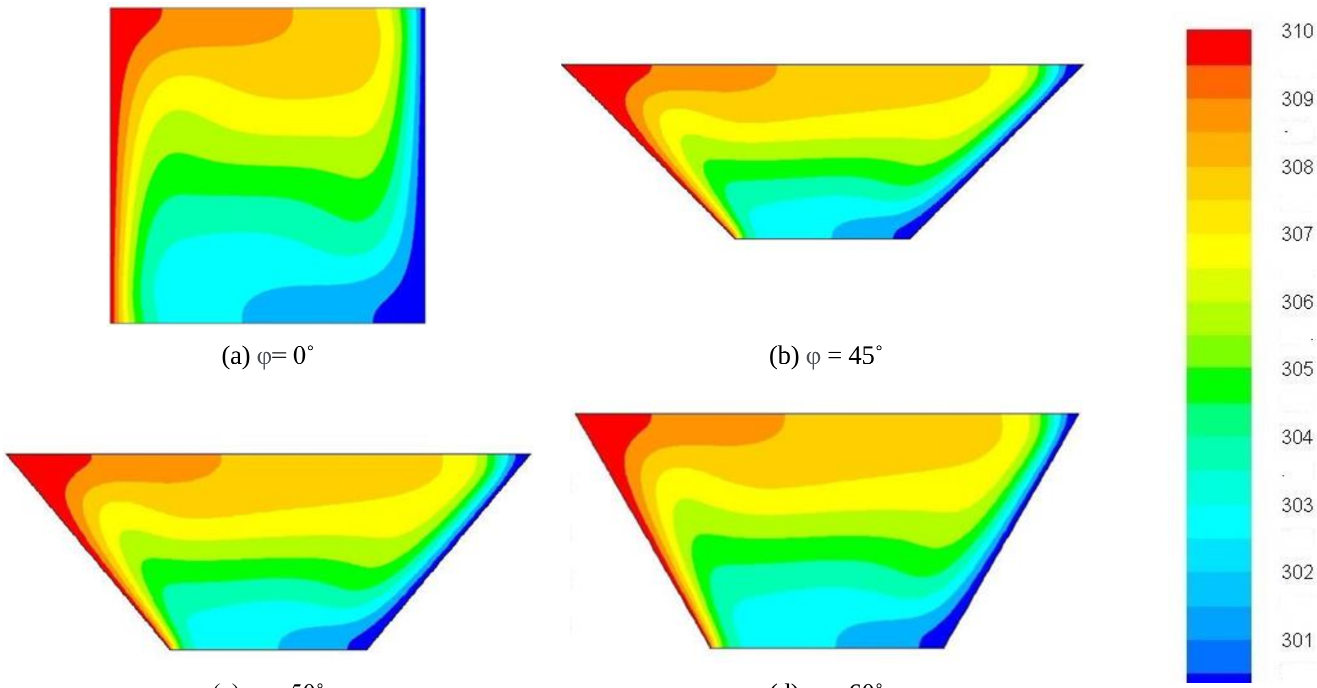


(a) φ= 0˚ (b) φ = 45˚

(c) φ = 50˚ (d) φ = 60˚

Fig. 6 Contour of the temperature of the square and trapezoid cavities for different inclination angles φ of (a) 0˚, (b) 45˚,(c) 50˚ and (d) 60˚ at Ra = $10^5$

Fig. 6(a) discusses the temperature of the square cavity (φ= 0˚) at Rayleigh number $10^5$. Fig. 6(b), (c), and (d) show the temperature of trapezoid cavities of different angles φ= 45˚, φ=50˚, φ=60˚ respectively at Rayleigh number $10^5$. It is seen that the temperature close to the left wall is higher than the right wall. It is due to the higher temperature of the wall at the left which is 310K than the wall at the right which is 300K. From all the figures, it is also observed that the temperature of the top wall is higher than the temperature of the bottom wall. It is because the temperature of the fluid near the left wall raised because of heating. Hence, fluid density decreases. Then this warm air travels to the top wall which results in higher temperature near the top wall than the bottom wall. Again, the temperature near the right wall is lower than the left wall due to the buoyancy effect. For the cooling effect, fluid density increases near the right wall, and fluid becomes heavier and colder near the right wall. From Fig. 5 and Fig. 6, it is observed that the temperature distribution at Rayleigh number $10^5$ is more elongated than the temperature distribution at Rayleigh number $10^6$.

Fig. 7 shows how the Nusselt number at the hot wall of the cavities varies with the Rayleigh number for different shapes and different inclination angles. Analysis of Fig. 7(a) reveals intriguing trends in Nusselt numbers concerning squared and trapezoid (φ = 50˚) cavities. Initially, at low Rayleigh numbers, both cavities exhibit little variations. However, with rising Rayleigh numbers, a distinctive shift occurs, causing a monotonic increase in Nusselt numbers for both shapes. As the Rayleigh number escalates further, a marked and considerable upsurge in the Nusselt numbers is observed. For instance, at a Rayleigh number of $10^3$, the Nusselt number for the squared cavity is 1.1179, significantly lower than 8.8558 at $10^6$. Similarly, for the trapezoid cavity, the Nusselt number climbs from 1.4771 at Ra=$10^3$ to 15.889 at Ra=$10^6$, signifying a notable increment. Remarkably, comparisons between the two cavities at identical Rayleigh numbers reveal the trapezoid cavity consistently yielding higher Nusselt numbers.

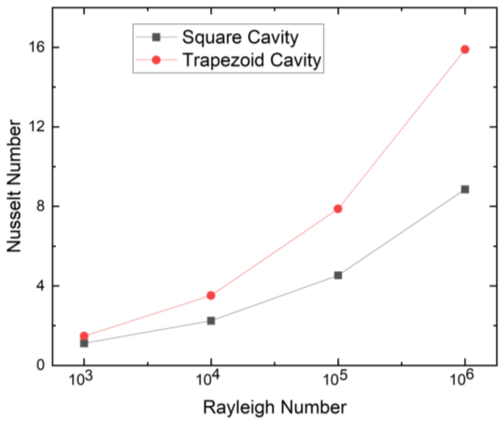


(a)

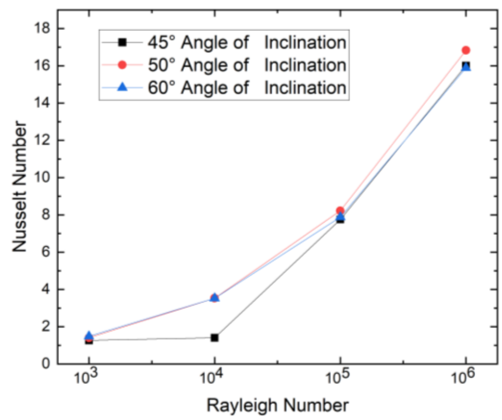


(b)

Fig. 7 Variation of Nusselt number with Rayleigh number for (a) different shape and (b) varying angle of inclination in trapezoid cavities

At lower Rayleigh numbers, the Nusselt number difference between the squared and trapezoid cavities is marginal but becomes more pronounced as the Rayleigh number increases.

Fig. 7(b) demonstrates how the angle of inclination affects the Nusselt number's behavior across different Rayleigh numbers. From the data the Nusselt number changes depending on the slope of the surface. At inclination angles φ =60˚ and φ =50˚, there's a similar trend in how the Nusselt number changes with increasing Rayleigh numbers. Initially, at lower Rayleigh numbers (Ra= $10^4$ to $10^5$), the Nusselt number grows slowly, but this increase becomes much more pronounced at higher Rayleigh numbers of Ra=$10^5$ to $10^6$. However, at an inclination angle of φ=45˚, the behavior of the Nusselt number is distinct from that observed at φ=60˚ and φ=50˚ at Ra=$10^4$. Specifically, at φ=50˚, the Nusselt number surpasses both φ=60˚ and φ=45˚ angles, indicating a better heat transfer efficiency. Hence, the enclosed trapezoid shape cavity with the inclination angle of φ=50˚ is the optimum consideration for laminar natural convection among the selection of the angles in the current study.

Fig. 8 and Fig. 9 explain velocity contour for squared and trapezoid cavities at Rayleigh number Ra = $10^6$ and Ra = $10^5$ respectively. In Fig. 8 and Fig. 9, the velocity varies with position inside the squared and trapezoid cavities. For the heating and cooling effects of natural convection, low-dense fluids move toward the top wall from the bottom wall and high-dense fluids move toward the top wall to the bottom wall respectively. From the numerical result, it is found that there is variation in velocity for different positions inside the trapezoid cavity due to the behavior of natural convection. As the Rayleigh number increases, velocity increases significantly. At a low Rayleigh number, velocity remains very low due to the behavior of natural convection. Velocity inside the cavity is created by some parts of the air being heavier than others. Due to the high temperature of the left wall, there occurs heating. For heating, the density of air near the left wall decreased. The air with reduced density moves relatively faster than the other air inside the cavity. Similarly, near the right wall, there occurs a cooling process. As a result, the air is heavier than the others in this region. Then, this heavier air moves down towards the bottom wall. For this density variation, velocity varies inside the cavity.

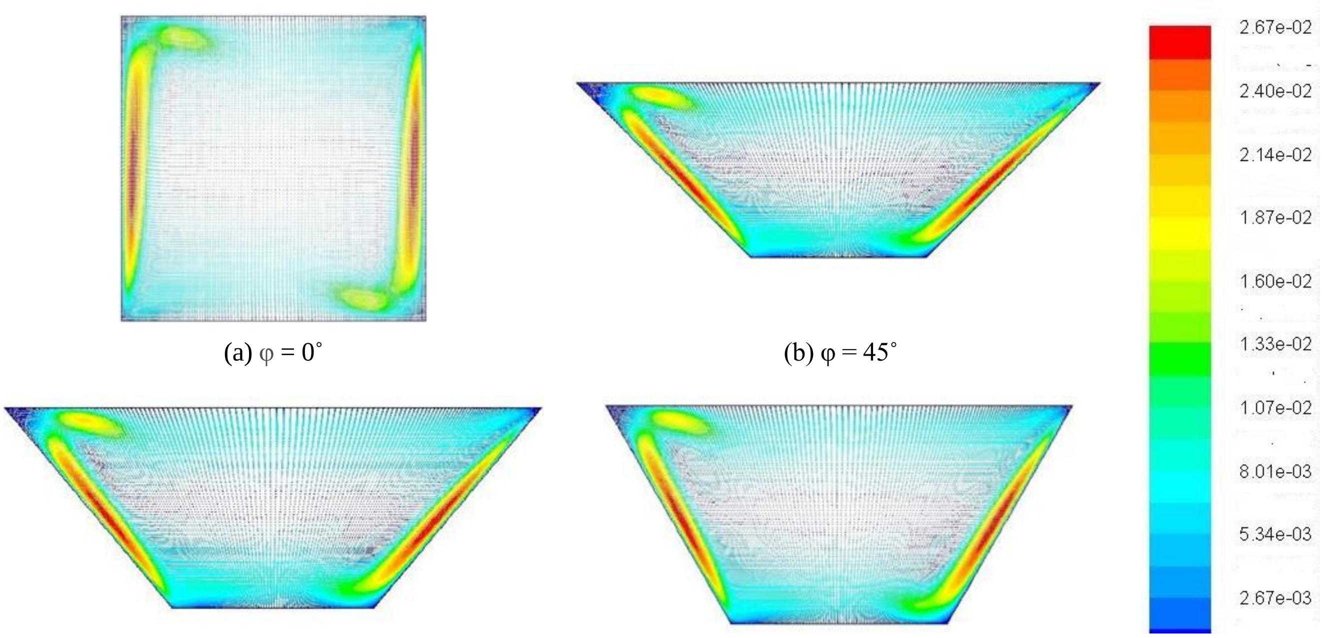


(a) φ = 0˚ (b) φ = 45˚ (c) φ = 50˚ (d) φ = 60˚

Fig. 8 Velocity contour of the square and trapezoid cavities for different inclination angle φ of (a) =0˚, (b) 45˚, (c) 50˚ and (d) 60˚at Ra = $10^6$

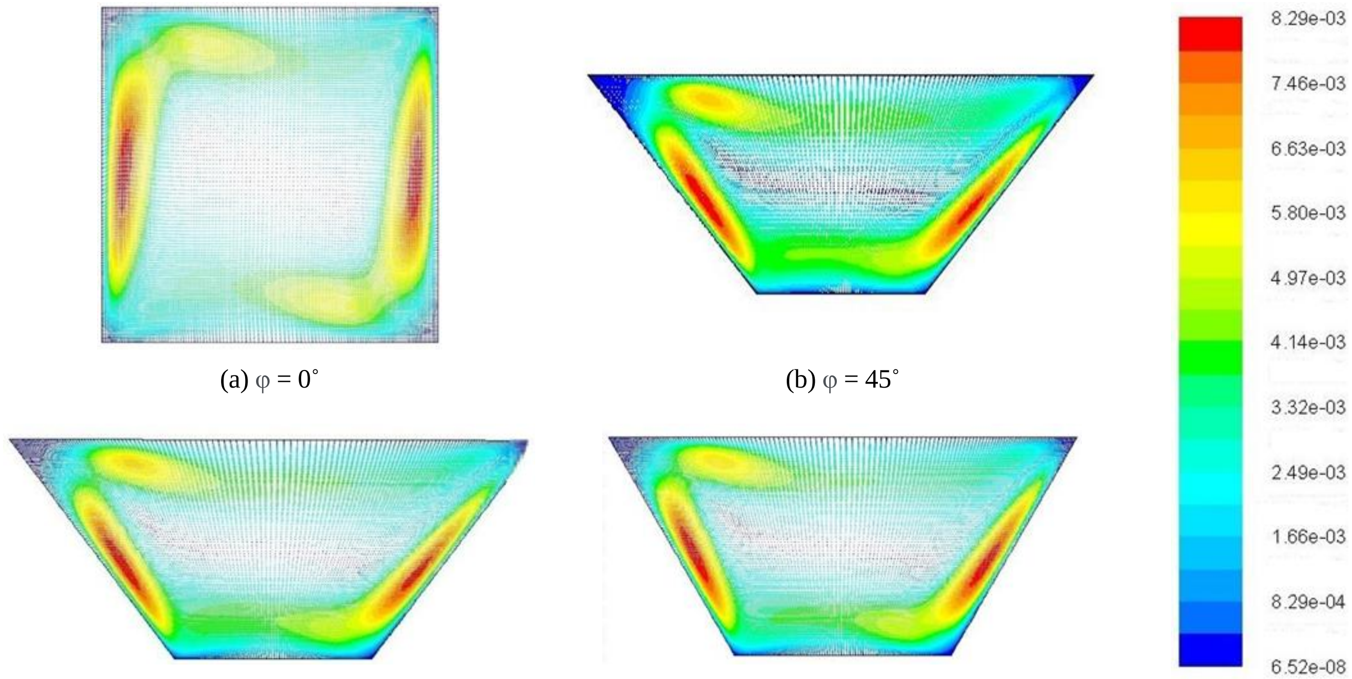


(a) φ = 0˚ (b) φ = 45˚ (c) φ = 50˚ (d) φ =60˚

Fig. 9 Velocity contour of the square and trapezoid cavities for different inclination angles φ of (a) =0˚, (b) 45˚, (c) 50˚ and (d) 60˚ at Ra = $10^5$

It is observed that points adjacent to the wall have the highest value because of the behavior of natural convection. In the points near the wall, heating and cooling occur. Heating occurs in the left wall, whose temperature is higher than that of the right wall. Due to high temperature, fluids take heat and become less dense. For variation in density, fluids with reduced density travel more quickly. Hence, in these points, fluids gain more velocity. Furthermore, at points far from walls, there is a lack of heat source for varying the density. So, inside the cavity at points far from the wall (almost in the middle of the cavities) fluids move less or none. Therefore, velocity becomes near to zero.

## 4 Conclusions

Different geometries for different shapes such as squared and trapezoid cavities and for different angles of inclination were analyzed numerically under natural convection conditions in this research. Four geometries were taken for study and numerically analyzed. The Nusselt number was measured, for all the geometries for both squared cavity and trapezoid cavity for various angles of inclination. From the result of the work, it is observed that the Nusselt number varies nonlinearly with the Rayleigh number. Nusselt number changes slowly at a low Ra number whereas the Nusselt number increases significantly and at a faster rate at a high Rayleigh number. The Nusselt number is also significantly affected by the shape of geometries. The Nusselt numbers for the trapezoid cavity are larger than the Nusselt numbers for the squared cavity at the same Rayleigh number. From numerical results, it is found that the temperature distribution at Ra = $10^5$ is wider than the temperature distribution at R = $10^6$. The velocity contours demonstrated the behavior of natural convection, showing zero velocity at the walls and higher velocity near the heated wall due to density variations. When compared to trapezoid cavities, the produced flow in the squared cavity is stronger due to the presence of an inclined wall inhibiting natural convection. Overall, these findings emphasize the significant impact of surface inclination on heat transfer efficiency, revealing diverse Nusselt number behaviors across different angles and Rayleigh numbers. Understanding these relationships is crucial for optimizing heat transfer in engineering and natural systems where inclined surfaces are involved.

**Nomenclature**

| Symbols | Meaning | Unit |
|---|---|---|
| $T_H$ | Hot wall Temperature | [K] |
| $T_C$ | Cold wall Temperature | [K] |
| g | Acceleration of gravity | [m/s$^2$] |
| Ra | Rayleigh number | [–] |
| k | Thermal conductivity | [W/m-K] |
| h | Convective heat transfer coefficient | [W/m$^2$K] |
| Nu | Nusselt number | [–] |
| α | Thermal diffusivity | [m$^2$/s] |
| β | Volumetric thermal expansion coefficient | [1/K] |
| ρ | Density | [kg/m$^3$] |
| υ | Kinematic viscosity | [m$^2$/s] |
| φ | Angle of inclination | [˚] |
| X, Y | Cartesian coordinates | [m] |
| p | Pressure | [Pa] |
| ρ | Absolute density of air | [kg/m$^3$] |

## References


[1] Adibi, T., Kangarluei, R.A. and Farhangmehr, V., 2017. Numerical study of natural convection flow inside squared and trapezoidal cavities in various conditions. *International Journal of Science, Engineering and Technology Research*, *6*(5), pp.2278-2298.

[2] de Vahl Davis, G., 1968. Laminar natural convection in an enclosed rectangular cavity. *International Journal of Heat and Mass Transfer*, *11*(11), pp.1675-1693.

[3] Sharif, M.A.R. and Liu, W., 2003. Numerical study of turbulent natural convection in a side-heated square cavity at various inclination angles. *Numerical Heat Transfer: Part A: Applications*, *43*(7), pp.693-716.

[4] Adibi, T. and Razavi, S.E., 2015. A new characteristic approach for incompressible thermo-flow in Cartesian and non-Cartesian grids. *International Journal for Numerical Methods in Fluids*, *79*(8), pp.371-393.

[5] Razavi, S.E. and Adibi, T., 2016. A novel multidimensional characteristic modeling of incompressible convective heat transfer. *Journal of Applied Fluid Mechanics*, *9*(3), pp.1135-1146.

[6] Akbari Kangarluei, R., 2015. Heat and mass transfer in industrial biscuit baking oven and effect of temperature on baking time. *Journal of Heat and Mass Transfer Research*, *2*(2), pp.79-90.

[7] Zaharuddin, S.D.A.S., Siri, Z., Saleh, H. and Hashim, I., 2020. Buoyant Marangoni convection of nanofluids in the right-angled trapezoidal cavity. *Numerical Heat Transfer, Part A: Applications*, *78*(11), pp.656-673.

[8] Alshomrani, A.S., Sivasankaran, S., Amer, A.A. and Biswas, A., 2019. Numerical study on convective flow in a three-dimensional enclosure with hot solid body and discrete cooling. *Numerical Heat Transfer, Part A: Applications*, *76*(2), pp.87-99.

[9] Yazdani, K., Sahebjamei, M. and Ahmadpour, A., 2019. Natural convection heat transfer and entropy generation in a porous trapezoidal enclosure saturated with power-law non-Newtonian fluids. *Heat Transfer Engineering, 41*(11), pp. 982-1001.

[10] Gowda, K.G.B.M., Rajagopal, M.S. and Seethramu, K.N., 2019. Numerical studies on natural convection in a trapezoidal enclosure with discrete heating. *Heat Transfer Engineering*, *41*(16), pp. 1-12.

[11] Sivarami Reddy, C., Ramachandra Prasad, V. and Jayalakshmi, K., 2021. Numerical simulation of natural convection heat transfer from a heated square cylinder in a square cavity filled with micropolar fluid. *Heat Transfer*, *50*(6), pp.5267-5285.

[12] Kishor, V., Singh, S. and Srivastava, A., 2018. Investigation of convective heat transfer phenomena in differentially-heated vertical closed cavity: Whole field experiments and numerical simulations. *Experimental Thermal and Fluid Science*, *99*, pp.71-84.

[13] Inam, M.I., 2020. Direct numerical simulation of laminar natural convection in a square cavity at different inclination angle. *Journal of Engineering Advancements*, *1*(01), pp.23-27.

[14] Ghalambaz, M., Doostani, A., Izadpanahi, E. and Chamkha, A.J., 2020. Conjugate natural convection flow of Ag–MgO/water hybrid nanofluid in a square cavity. *Journal of Thermal Analysis and Calorimetry*, *139*, pp.2321-2336.

[15] Nadeem, S., Haider, J.A., Akhtar, S. and Ali, S., 2022. Numerical simulations of convective heat transfer of a viscous fluid inside a rectangular cavity with heated rotating obstacles. *International Journal of Modern Physics B*, *36*(28), p.2250200.

[16] Saleh, H., Roslan, R. and Hashim, I., 2011. Natural convection heat transfer in a nanofluid-filled trapezoidal enclosure. *International Journal of Heat and Mass Transfer*, *54*(1-3), pp.194-201.

[17] Saha, S.C., Patterson, J.C. and Lei, C., 2010. Natural convection in attics subject to instantaneous and ramp cooling boundary conditions. *Energy and Buildings*, *42*(8), pp.1192-1204.

[18] de Vahl Davis, G. and Jones, I., 1983. Natural convection in a square cavity: a comparison exercise. *International Journal for Numerical Methods in Fluids*, *3*(3), pp.227-248.

[19] Fusegi, T., Hyun, J.M., Kuwahara, K. and Farouk, B., 1991. A numerical study of three-dimensional natural convection in a differentially heated cubical enclosure. *International Journal of Heat and Mass Transfer*, *34*(6), pp.1543-1557.

[20] Khanafer, K., Vafai, K. and Lightstone, M., 2003. Buoyancy-driven heat transfer enhancement in a two-dimensional enclosure utilizing nanofluids. *International Journal of Heat and Mass Transfer*, *46*(19), pp.3639-3653.

[21] Bilgen, E., 2005. Natural convection in cavities with a thin fin on the hot wall. *International Journal of Heat and Mass Transfer*, *48*(17), pp.3493-3505.

[22] Lai, F.H. and Yang, Y.T., 2011. Lattice Boltzmann simulation of natural convection heat transfer of Al2O3/water nanofluids in a square enclosure. *International Journal of Thermal Sciences*, *50*(10), pp.1930-1941.

[23] Kobra, F., Quddus, N. and Alim, M.A., 2014. Heat transfer enhancement of Cu-water nanofluid filled in a square cavity with a circular disk under a magnetic field. *Procedia Engineering*, *90*, pp.582-587.